Supporting Information

Enhanced water splitting kinetics using $MgFeO_3$/MXene/VS_2 hybrid bifunctional catalysts

Sajjad Hussain[a,b], Dhanasekaran Vikraman[c], Zulfqar Ali Sheikh[d], Sikandar Aftab[e], Ghazanfar Nazir[b], Shoyebmohamad F. Shaikh[f], Deok-Kee Kim[d], Hyun-Seok Kim[c,*], Jongwan Jung[a,b,*]

[a] Hybrid Materials Center (HMC), Sejong University, Seoul 05006, Republic of Korea.

[b] Department of Nanotechnology and Advanced Materials Engineering, Sejong University, Seoul 05006, Republic of Korea.

[c] Division of Electronics and Electrical Engineering, Dongguk University-Seoul, Seoul 04620, Republic of Korea.

[d] Department of Convergence Engineering for Intelligent Drone and Department of Electrical Engineering, Sejong University, Seoul 05006, Republic of Korea.

[e] Department of Intelligent Mechatronics Engineering, Sejong University, Seoul 05006, Republic of Korea

[f] Department of Chemistry, College of Science, King Saud University, P.O. Box 2455, Riyadh 11451, Saudi Arabia

*Corresponding authors' Email: hyunseokk@dongguk.edu (H.S.K); jwjung@sejong.ac.kr (J.J)

S1. Electrode preparation

All electrocatalytic experiments were conducted with a PARSTAT MC (PMC-200) workstation at a sweep rate of 10 mV/s, utilizing a standard three-electrode setup in 1 M KOH electrolyte for the HER, OER and overall water splitting tests at room temperature. Working electrodes were prepared by homogenizing active materials (MFO, MFO/MXene, MFO/VS_2, and MFO/MXene/VS_2) with poly(vinylidene fluoride) and carbon black in an 80:10:10 ratio, respectively, using N-methyl-2-pyrrolidone as the solvent. This slurry was coated onto nickel foam (NF) substrates and thermally treated at 100 °C for 12 hours to remove contaminants and solvent, achieving a consistent loading of 3 mg of active material. In the HER and OER experiments, the active materials functioned as the working electrodes, with a Hg/HgO electrode as the reference and a graphite rod as the counter electrode in an alkaline medium. Electrochemical impedance spectroscopy (EIS) was performed over a frequency range of 10 mHz to 100 kHz with a 10 mV potential amplitude. Water-splitting reactions were evaluated in device configurations of MFO/MXene/VS_2‖MFO/MXene/VS_2 and Pt/C‖RuO_2, with EIS conducted in a 1 M KOH solution. iR correction for ohmic resistance losses was applied during polarization studies, and electrode potentials were referenced to the reversible hydrogen electrode (RHE) using the equation: $E(RHE)_{HgO} = E(vs.\ Hg/HgO) + E^0{}_{(Hg/HgO)} + 0.0592 \times pH$.

S2. Characterization Techniques

XRD patterns were obtained using a Rigaku X-ray diffractometer with Cu-Kα radiation (0.154 nm) at 40 kV and 40 mA, scanning from 5-80° (2θ). The morphological properties and elemental mapping/analysis of the prepared nanostructures were characterized using field-emission scanning electron microscopy (HITACHI S-4700) and transmission electron microscopy

(JEOL JEM-2100F, 200 kV). Raman spectroscopy measurements were conducted at room temperature with a Renishaw Invia RE04, employing a 512 nm Ar laser with a 30-second exposure time. XPS measurements were performed using an Ulvac PHI X-tool spectrometer with Al Kα X-ray radiation (1486.6 eV).

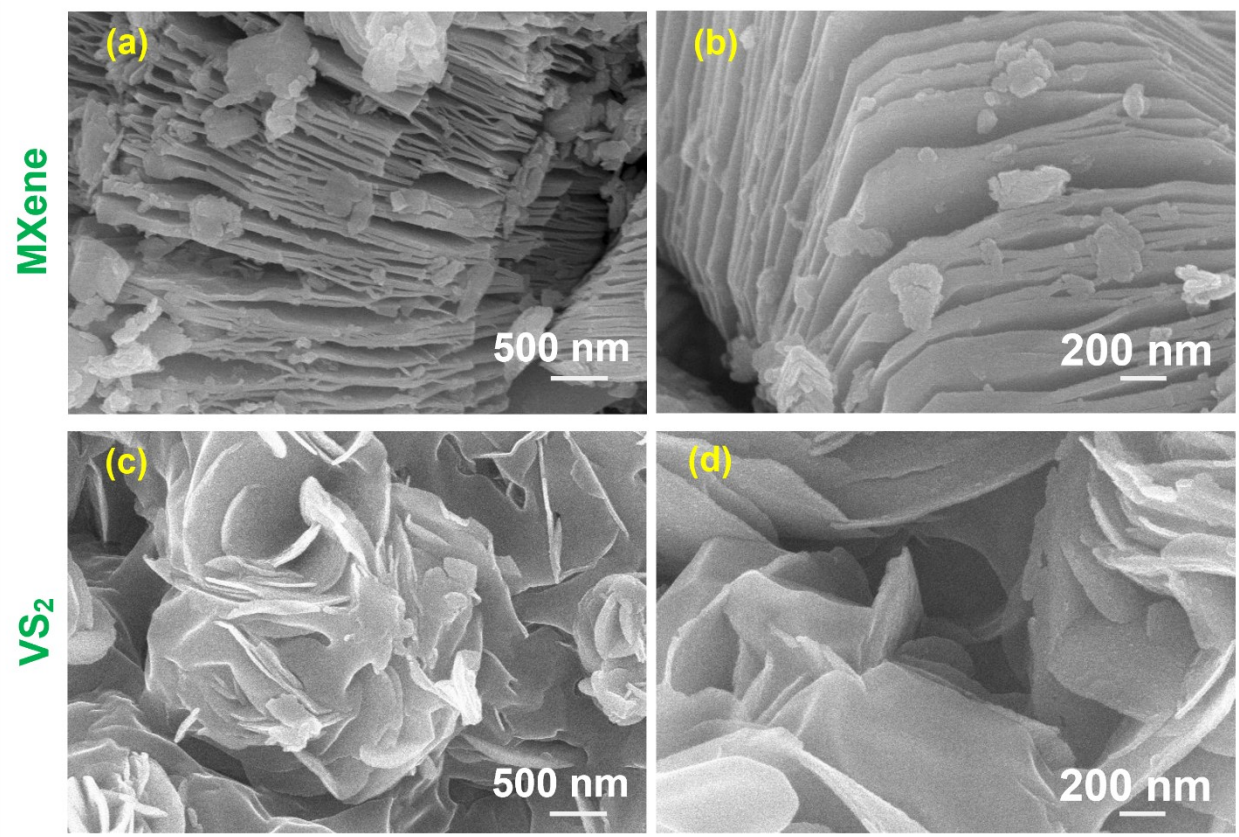

Figure S1. Field emission scanning electron microscopy (FESEM) images showing the morphological characteristics of (a-b) MXene and (c-d) VS_2.

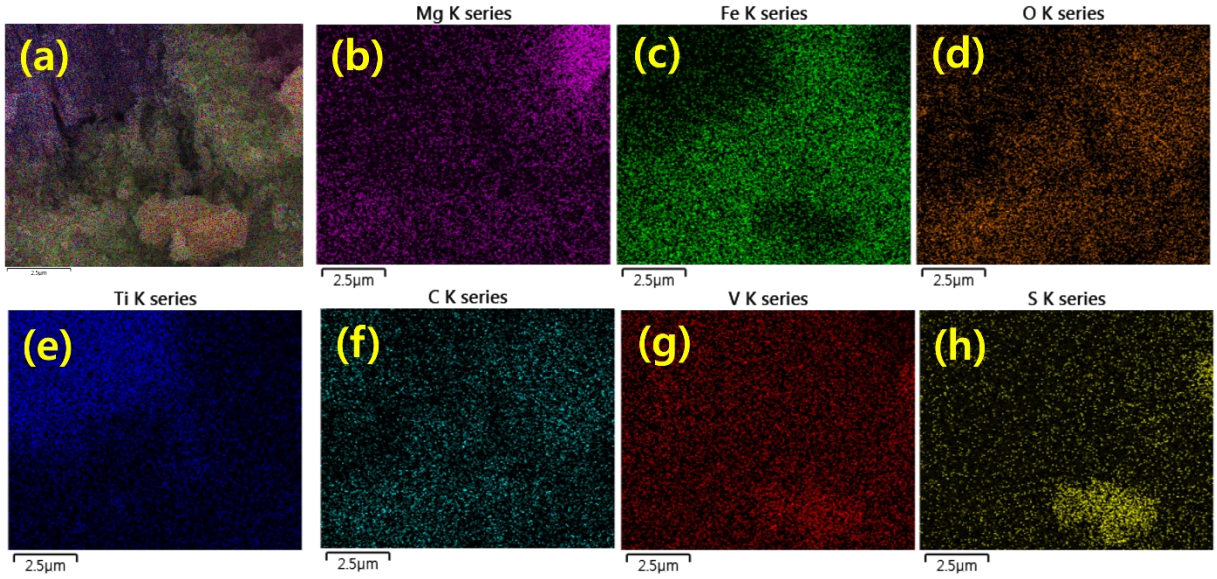

Figure S2. (a) FESEM mapping image of MFO/MXene/VS_2 hybrid composite and (b-h) their elemental mapping images ((b) Mg; (c) Fe; (d) O; (e) Ti; (f) C; (g) V and (g) S).

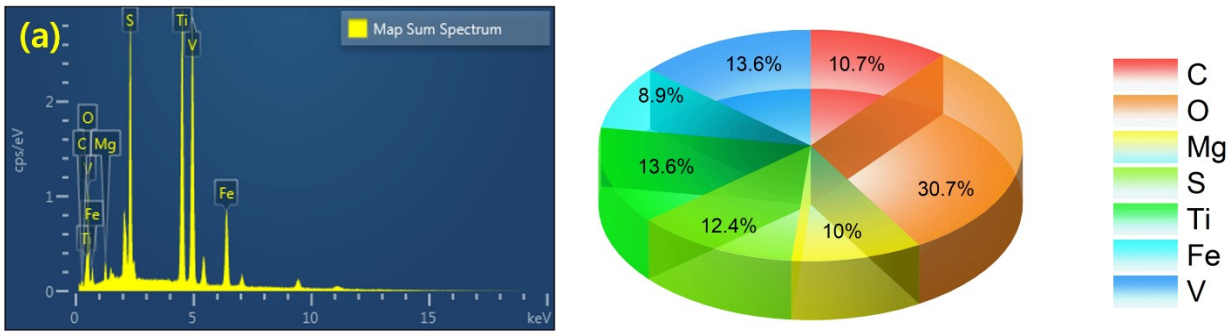

Figure S3. (a) Energy dispersive X-ray spectroscopy (EDS) pattern and (b) the composition of MFO/MXene/VS_2 hybrid.

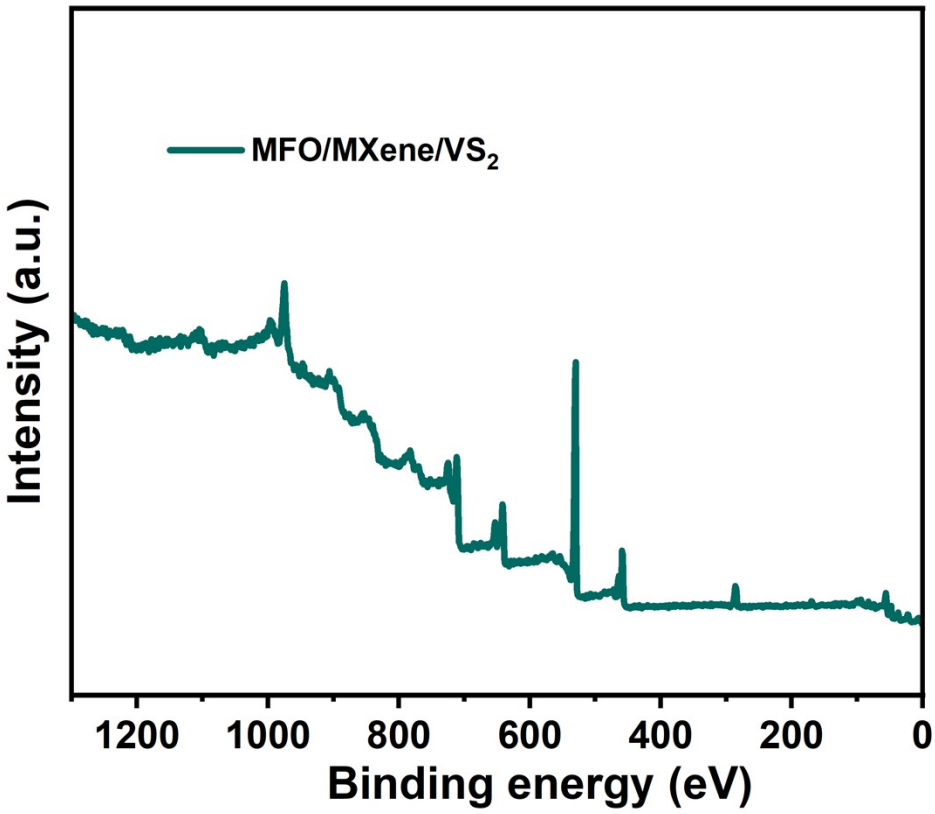

Figure S4. X-ray photoelectron spectroscopy (XPS) survey profile of the MFO/MXene/VS_2 hybrid

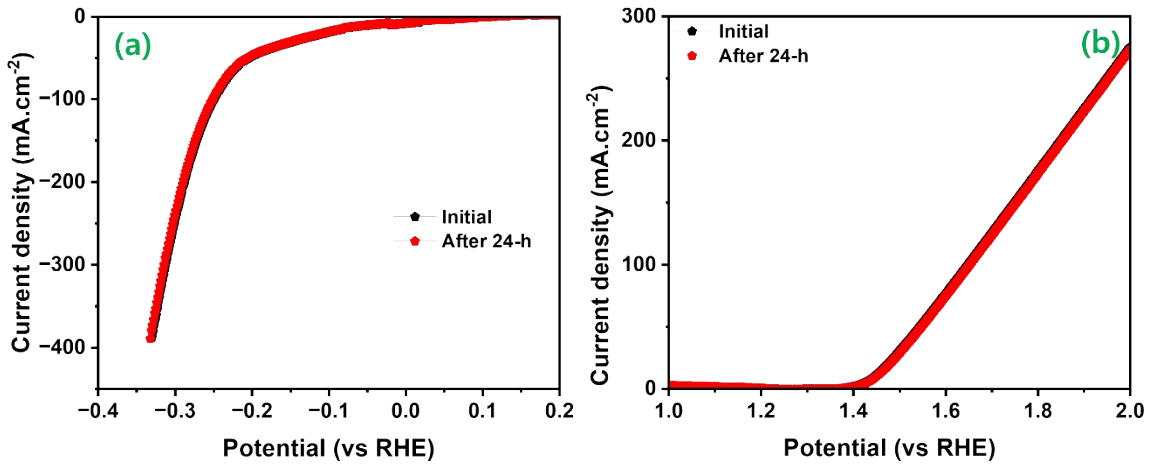

Figure S5. Linear sweep voltammetry (LSV) curves of MFO/MXene/VS_2 hybrid composite before and after 24-h working operation in 1 M KOH electrolyte solution.

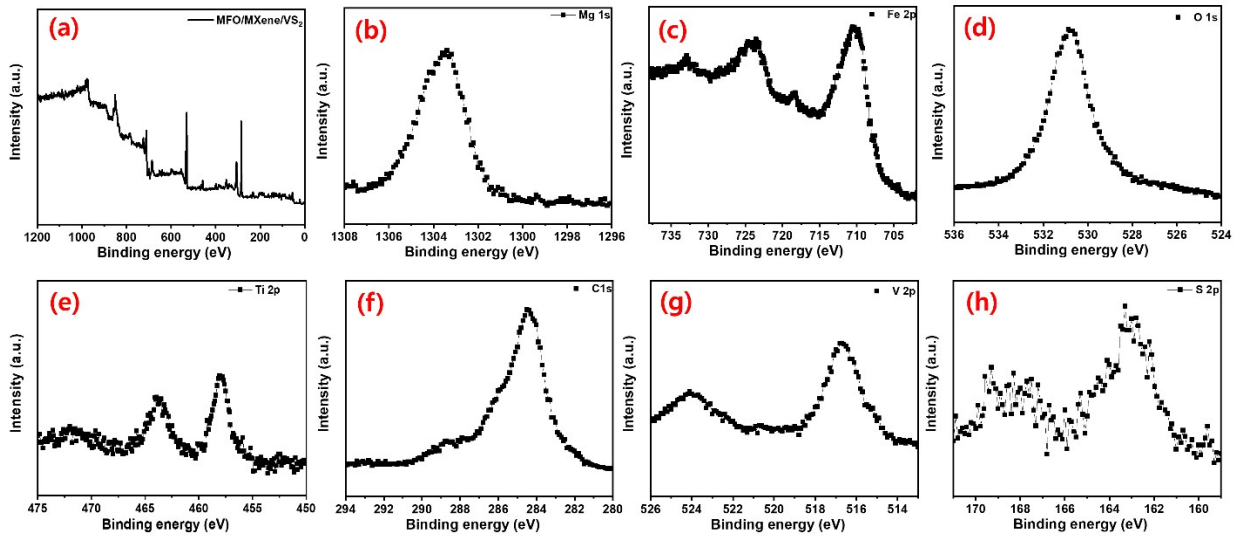

Figure S6. High-resolution X-ray photoelectron spectroscopy (XPS) profiles after 24-h overall water splitting process: (a) survey scan, (b) Mg 1s, (c) Fe 2p, (d) O 1s, (e) Ti 2p, (f) C 1s, (g) V 2p, and (h) S 2p regions of MFO/MXene/VS_2 hybrid composites.

Table S1. HER catalytic performances of the TMDs and MXene-based electrocatalysts

Electrocatalyst	Electrolyte	η (mV)	Synthesis Method	Morphology	Tafel Slope ($mV \cdot dec^{-1}$)	Ref
$MgFeO_3$@MXene@VS_2	***1M KOH***	***34 @ 10 mA/cm^2***	***Hydrothermal synthesis***	***Nano-cubes integrated hybrid nanosheets***	***62***	***This work***
FeNi@MXene ($Mo_2TiC_2T_x$)	1M KOH	160@ 10 mA/cm^2	Solvothermal reaction	FeS_2 nanoparticles anchored on nanosheets	103.46	[1]
MoS_2@Mo_2CTx	0.5M H_2SO_4	176@10 mA/cm^2	Etching + Hydrothermal	2D organ	207	[2]
Co-MoS_2@Mo_2CTx	1M KOH	112@10 mA/cm	Etching + Tube furnace	bulk morphology	82	[3]
NiFe-LDH/MXene-RGO	1M KOH	362@10 mA/cm^2	Etching + Hydrothermal	3D porous skeletons	100	[4]
WS_2/W_2C heterostructure	0.5 M H_2SO_4	126@ 10 mA/cm^2	CVD	Nano-sheet	68	[5]
MoS_2/Ti_3C_2-MXene@C	0.5 M H_2SO_4	135@ 10 mA/cm^2	Etching + Tube furnace	Flower+ 3D porous	45	[6]
WS_2/Ti_3C_2	0.5 M H_2SO_4	150@ 10 mA/cm^2	Etching + Hydrothermal	accordion-multilayer+ nanosheets	62	[7]
MoS_2/MXene heterostructures	0.5 M H_2SO_4	280@ 10 mA/cm^2	Etching + Hydrothermal	accordion-multilayer+ coarse and uneven	68	[8]
MoO_2/α-Mo_2C heterojunction	0.5 M H_2SO_4 and 1.0 M KOH	152 & -100@ 10 mA/cm^2	CVD	core-shell structure	65 & 50	[9]
Ti_2NT_x@MOF-CoP	1M KOH	112@10 mA/cm^2	freeze-drying+ tube furnace	cubic-like layered ultrathin	67.1	[10]
$NiSe_2/Ti_3C_2T_x$ hybrid	0.5 M H_2SO_4	200 mV @10 mA g^{-1}	Etching + Hydrothermal	Octahedral structure	37.7	[11]
MoS_2/ Mo_2C-NCNTs	0.5 M H_2SO_4	145@ 10 mA/cm^2	Etching + Hydrothermal	Hierarchical1D nanostructure	69	[12]
WS_2–$Ti_3C_2T_x$	0.5 M H_2SO_4	66@ 10 mA/cm^2	Etching + Hydrothermal	wrinkled nanosheets	46.7	[13]
Mo_2C Nanoparticles/ Graphitic CC	0.5 M H_2SO_4	200@ 10 mA/cm^2	CVD	Nanoparticles porous nanofibers	62.6	[14]
MoP/Mo_2C@C	0.5 M H_2SO_4	89@ 10 mA/cm^2	Tube furnace	Nanoparticles	45	[15]
V-$Ti_4N_3T_x$	0.5 M H_2SO_4	330 @ 10 mA/cm^2	oxygen-assisted molten salt	multilayer flakes	190	[16]
BNNS@Ti_3C_2	0.5M H_2SO_4	52@10 mA/cm	ball-milling+ tube furnace	multilayer broken flakes	39	[17]
Ni/β-Mo_2C	0.5 M H_2SO_4	155 @ 10 mA/cm^2	tube furnace	irregular shaped	79	[18]

Table S2. OER catalytic performances of the TMDs and MXene-based electrocatalysts

Electrocatalyst	Electrolyte	η (mV)	Synthesis Method	Morphology	Tafel Slope ($mV \cdot dec^{-1}$)	Ref
$CoNiO_2$@MoS_2	***1M KOH***	***220 @ 10 mA/cm^2***	***Hydrothermal synthesis***	***Nano-cubes integrated hybrid nanosheets***	***44***	***This work***
FeNi@MXene ($Mo_2TiC_2T_x$)	1M KOH	190@ 10 mA/cm^2	Solvothermal reaction	FeS_2 nanoparticles anchored on nanosheets	42.78	[1]
Ti_2NT_x@MOF-CoP	1M KOH	241@50 mA/cm	freeze-drying+ tube furnace	cubic-like layered ultrathin	96.7	[10]
FeNi-LDH/Ti_3C_2-MXene	1M KOH	250 @ 10 mA/cm^2	Etching + freeze-drying	3D porous network	42	[19]
CoP/Mo_2CT_x	1M KOH	260@10 mA/cm	Etching + tube furnace	accordion-multilayer+ nanosheets	51	[20]
NiFeP/MXene	1M KOH	286@50 mA/cm	Etching + Hydrothermal	3D laminar structures	35	[21]
Ti_3C_2Tx/TiO_2/NiFeCo-LDH	1M KOH	155 @ 10 mA/cm^2	Etching + Hydrothermal	Accordion + spindle like morphology	98.4	[22]
NiFe LDH/$Ti_3C_2T_x$/NF	1M KOH	200@10 mA/cm	Etching + Hydrothermal	Hollow petal shape structures	64.2	[23]
CoFe-LDH on MXene	1M KOH	319 @ 10 mA/cm^2	Etching + Hydrothermal	Accordion+ densely packed arrays	50	[24]
CoS_2@MXene	1M KOH	150@ 10 mA/cm^2	Etching + freeze-drying	NWs anchored on MXene	92	[25]
FeS_2@MXene	1M KOH	240@ 10 mA/cm^2	Etching + solvothermal reaction	nanoparticles anchored on MXene	58.7	[26]
CoNi-ZIF-67@Ti_3C_2Tx	1M KOH	275@ 10 mA/cm^2	Etching + chemical reaction	rhombic dodecahedral structure on MXene	65.1	[27]
MWCNT/V_2CT_x	1M KOH	469@ 10 mA/cm^2	Etching + sonication	MWCNTs on accordion-like structure	77	[28]
Fe_3O_4/$Ti_3C_2T_x$	1M KOH	290@ 10 mA/cm^2	Etching + Hydrothermal	sparsely and unevenly nanoplates grown on MXene	65.1	[29]
Co-CoO/Ti_3C_2-MXene/NF	1M KOH	271@10 mA/cm	Etching + vacuum tube furnace	Co-CoO nanoplates on thin MXene nanosheets	47	[30]
CoP@MXene	1M KOH	146@ 10 mA/cm^2	Etching + Hydrothermal	1D CoP nanorods on MXene nanosheets	32.5	[31]

$NiSe_2$@MoS_2	1 M KOH	267 @ 10 mA/cm^2	electrochemical deposition + hydrothermal synthesis	Disorder nanograin	85	[32]
Co^{3+}–Cr_2CT_x	1M KOH	420@ 10 mA/cm^2	E-etching method	3D polydisperse composites	-	[33]

References

1. J. Wang, P. He, Y. Shen, L. Dai, Z. Li, Y. Wu and C. An, FeNi nanoparticles on Mo2TiC2Tx MXene@ nickel foam as robust electrocatalysts for overall water splitting, *Nano Research*, 2021, **14**, 3474-3481.
2. J. Ren, H. Zong, Y. Sun, S. Gong, Y. Feng, Z. Wang, L. Hu, K. Yu and Z. Zhu, 2D organ-like molybdenum carbide (MXene) coupled with MoS 2 nanoflowers enhances the catalytic activity in the hydrogen evolution reaction, *CrystEngComm*, 2020, **22**, 1395-1403.
3. J. Liang, C. Ding, J. Liu, T. Chen, W. Peng, Y. Li, F. Zhang and X. Fan, Heterostructure engineering of Co-doped MoS 2 coupled with Mo 2 CT x MXene for enhanced hydrogen evolution in alkaline media, *Nanoscale*, 2019, **11**, 10992-11000.
4. B. Shen, H. Huang, Y. Jiang, Y. Xue and H. He, 3D interweaving MXene–graphene network–confined Ni–Fe layered double hydroxide nanosheets for enhanced hydrogen evolution, *Electrochimica Acta*, 2022, 139913.
5. Y. Li, X. Wu, H. Zhang and J. Zhang, Interface Designing over WS2/W2C for Enhanced Hydrogen Evolution Catalysis, *ACS Applied Energy Materials*, 2018, **1**, 3377-3384.
6. X. Wu, Z. Wang, M. Yu, L. Xiu and J. Qiu, Stabilizing the MXenes by carbon nanoplating for developing hierarchical nanohybrids with efficient lithium storage and hydrogen evolution capability, *Advanced Materials*, 2017, **29**, 1607017.
7. M. A. Tekalgne, H. H. Do, T. V. Nguyen, Q. V. Le, S. H. Hong, S. H. Ahn and S. Y. Kim, MXene Hybrid Nanosheet of WS2/Ti3C2 for Electrocatalytic Hydrogen Evolution Reaction, *ACS Omega*, 2023.
8. L. Huang, L. Ai, M. Wang, J. Jiang and S. Wang, Hierarchical MoS2 nanosheets integrated

Ti3C2 MXenes for electrocatalytic hydrogen evolution, *International Journal of Hydrogen Energy*, 2019, **44**, 965-976.

9. Y. Liu, B. Huang and Z. Xie, Hydrothermal synthesis of core-shell MoO2/α-Mo2C heterojunction as high performance electrocatalyst for hydrogen evolution reaction, *Applied Surface Science*, 2018, **427**, 693-701.
10. H. Zong, R. Qi, K. Yu and Z. Zhu, Ultrathin Ti2NTx MXene-wrapped MOF-derived CoP frameworks towards hydrogen evolution and water oxidation, *Electrochimica Acta*, 2021, **393**, 139068.
11. H. Jiang, Z. Wang, Q. Yang, L. Tan, L. Dong and M. Dong, Ultrathin Ti 3 C 2 T x (MXene) nanosheet-wrapped NiSe 2 octahedral crystal for enhanced supercapacitor performance and synergetic electrocatalytic water splitting, *Nano-micro letters*, 2019, **11**, 1-14.
12. K. Zhang, Y. Zhao, S. Zhang, H. Yu, Y. Chen, P. Gao and C. Zhu, MoS 2 nanosheet/Mo 2 C-embedded N-doped carbon nanotubes: synthesis and electrocatalytic hydrogen evolution performance, *Journal of Materials Chemistry A*, 2014, **2**, 18715-18719.
13. F. Rasool, B. M. Pirzada, S. H. Talib, T. Alkhidir, D. H. Anjum, S. Mohamed and A. Qurashi, In Situ Growth of Interfacially Nanoengineered 2D–2D WS2/Ti3C2T x MXene for the Enhanced Performance of Hydrogen Evolution Reactions, *ACS applied materials & interfaces*, 2024, **16**, 14229-14242.
14. H. Wang, C. Sun, Y. Cao, J. Zhu, Y. Chen, J. Guo, J. Zhao, Y. Sun and G. Zou, Molybdenum carbide nanoparticles embedded in nitrogen-doped porous carbon nanofibers as a dual catalyst for hydrogen evolution and oxygen reduction reactions, *Carbon*, 2017, **114**, 628-634.
15. L.-N. Zhang, S.-H. Li, H.-Q. Tan, S. U. Khan, Y.-Y. Ma, H.-Y. Zang, Y.-H. Wang and Y.-G. Li, MoP/Mo2C@ C: a new combination of electrocatalysts for highly efficient hydrogen evolution over the entire pH range, *ACS applied materials & interfaces*, 2017, **9**, 16270-16279.
16. A. Djire, X. Wang, C. Xiao, O. C. Nwamba, M. V. Mirkin and N. R. Neale, Basal plane hydrogen evolution activity from mixed metal nitride MXenes measured by scanning electrochemical microscopy, *Advanced Functional Materials*, 2020, **30**, 2001136.
17. Z. Ai, B. Chang, C. Xu, B. Huang, Y. Wu, X. Hao and Y. Shao, Interface engineering in the BNNS@ Ti 3 C 2 intercalation structure for enhanced electrocatalytic hydrogen evolution,

New Journal of Chemistry, 2019, **43**, 8613-8619.

18. T. Ouyang, A.-N. Chen, Z.-Z. He, Z.-Q. Liu and Y. Tong, Rational design of atomically dispersed nickel active sites in β-Mo_2C for the hydrogen evolution reaction at all pH values, *Chem. Comm.*, 2018, **54**, 9901-9904.
19. M. Yu, S. Zhou, Z. Wang, J. Zhao and J. Qiu, Boosting electrocatalytic oxygen evolution by synergistically coupling layered double hydroxide with MXene, *Nano Energy*, 2018, **44**, 181-190.
20. S. Liu, Z. Lin, R. Wan, Y. Liu, Z. Liu, S. Zhang, X. Zhang, Z. Tang, X. Lu and Y. Tian, Cobalt phosphide supported by two-dimensional molybdenum carbide (MXene) for the hydrogen evolution reaction, oxygen evolution reaction, and overall water splitting, *Journal of Materials Chemistry A*, 2021, **9**, 21259-21269.
21. J. Chen, Q. Long, K. Xiao, T. Ouyang, N. Li, S. Ye and Z.-Q. Liu, Vertically-interlaced NiFeP/MXene electrocatalyst with tunable electronic structure for high-efficiency oxygen evolution reaction, *Science Bulletin*, 2021, **66**, 1063-1072.
22. N. Hao, Y. Wei, J. Wang, Z. Wang, Z. Zhu, S. Zhao, M. Han and X. Huang, In situ hybridization of an MXene/TiO 2/NiFeCo-layered double hydroxide composite for electrochemical and photoelectrochemical oxygen evolution, *RSC advances*, 2018, **8**, 20576-20584.
23. Z. Li, X. Wang, J. Ren and H. Wang, NiFe LDH/Ti3C2Tx/nickel foam as a binder-free electrode with enhanced oxygen evolution reaction performance, *International Journal of Hydrogen Energy*, 2022, **47**, 3886-3892.
24. C. Hao, Y. Wu, Y. An, B. Cui, J. Lin, X. Li, D. Wang, M. Jiang, Z. Cheng and S. Hu, Interface-coupling of CoFe-LDH on MXene as high-performance oxygen evolution catalyst, *Materials Today Energy*, 2019, **12**, 453-462.
25. S. Han, Y. Chen, Y. Hao, Y. Xie, D. Xie, Y. Chen, Y. Xiong, Z. He, F. Hu and L. Li, Multi-dimensional hierarchical CoS2@ MXene as trifunctional electrocatalysts for zinc-air batteries and overall water splitting, *Science China Materials*, 2021, **64**, 1127-1138.
26. S. Peng, Y. Xie, H. Yu, L. Deng, D. Yu, L. Li, R. Amin, A. E. Fetohi, M. Y. Maximov and K. El-Khatib, Anchoring stable FeS2 nanoparticles on MXene nanosheets via interface engineering for efficient water splitting, *Inorganic Chemistry Frontiers*, 2022.
27. Y. Wen, Z. Wei, C. Ma, X. Xing, Z. Li and D. Luo, MXene boosted CoNi-ZIF-67 as highly

efficient electrocatalysts for oxygen evolution, *Nanomaterials*, 2019, **9**, 775.

28. S. A. Zahra and S. Rizwan, MWCNT-modified MXene as cost-effective efficient bifunctional catalyst for overall water splitting, *RSC advances*, 2022, **12**, 8405-8413.
29. L. Zhang, Z. Wang, W. Chen, R. Yuan, K. Zhan, M. Zhu, J. Yang and B. Zhao, Fe 3 O 4 nanoplates anchored on Ti 3 C 2 T x MXene with enhanced pseudocapacitive and electrocatalytic properties, *Nanoscale*, 2021, **13**, 15343-15351.
30. D. Guo, X. Li, Y. Jiao, H. Yan, A. Wu, G. Yang, Y. Wang, C. Tian and H. Fu, A dual-active Co-CoO heterojunction coupled with Ti3C2-MXene for highly-performance overall water splitting, *Nano Research*, 2022, **15**, 238-247.
31. N. C. S. Selvam, J. Lee, G. H. Choi, M. J. Oh, S. Xu, B. Lim and P. J. Yoo, MXene supported Co x A y (A= OH, P, Se) electrocatalysts for overall water splitting: unveiling the role of anions in intrinsic activity and stability, *Journal of Materials Chemistry A*, 2019, **7**, 27383-27393.
32. Y. Huang, J. Huang, K. Xu and R. Geng, Constructing NiSe 2@ MoS 2 nano-heterostructures on a carbon fiber paper for electrocatalytic oxygen evolution, *RSC advances*, 2021, **11**, 26928-26936.
33. S.-Y. Pang, Y.-T. Wong, S. Yuan, Y. Liu, M.-K. Tsang, Z. Yang, H. Huang, W.-T. Wong and J. Hao, Universal strategy for HF-free facile and rapid synthesis of two-dimensional MXenes as multifunctional energy materials, *Journal of the American Chemical Society*, 2019, **141**, 9610-9616.